Engaging a Non-Catalytic Cysteine Residue Drives Unprecedented Selectivity of Caspase Inhibition

Kurt S. Van Horn,[†,‡] Dongju Wang,[†,#,‡] Daniel Medina-Cleghorn,[†] Peter S. Lee,[†] Clifford Bryant,[†] Chad Altobelli, [†] Priyadarshini Jaishankar, [†] Kevin K. Leung, [†] Raymond A. Ng,[§] Andrew J. Ambrose, [†] Yinyan Tang,[†] Michelle R. Arkin,[†,*] and Adam R. Renslo[†,*]

[†]Department of Pharmaceutical Chemistry, University of California, San Francisco, 600 16th Street, San Francisco, California 94143, United States

[#]School of Pharmaceutical Sciences, Tsinghua University, Beijing, China

[§]Chempartner Corporation, 280 Utah Avenue, South San Francisco, California 94080, United States

ABSTRACT: The caspases are a family of cysteine dependent proteases with important cellular functions in inflammation and apoptosis, while also implicated in human disease. Classical chemical tools to study caspase function lack selectivity for specific caspase family members due to highly conserved active sites and catalytic machinery. To overcome this limitation, we targeted a non-catalytic cysteine residue (C264) unique to Caspase-6, an enigmatic and understudied caspase isoform. Starting from disulfide ligands identified in a cysteine trapping screen, we used structure-informed covalent ligand design to produce potent, irreversible inhibitors (e.g., **3a**) and chemoproteomic probes (e.g., **13-*t***) of Caspase-6 that exhibit unprecedented selectivity over other caspase family members and high proteomic selectivity. This approach and the new tools described will enable rigorous interrogation of the role of Caspase-6 in developmental biology and in inflammatory and neurodegenerative diseases.

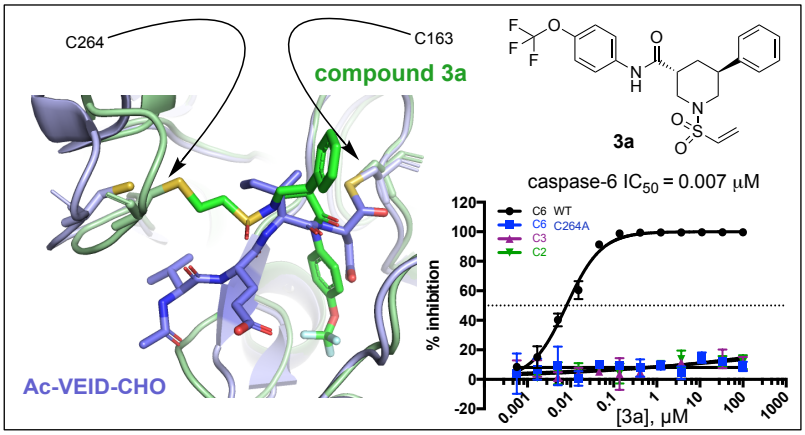

Caspases are cysteine-dependent aspartyl-specific proteases involved in a range of cellular and disease processes ranging from apoptosis to inflammation and neurodegeneration.[1–5] Caspase family members are broadly classified as inflammatory (C1, C4, and C5) or apoptotic caspases. The apoptotic caspases include so-called initiator caspases (C8 and C9) that cleave executioner caspases (C3, C6, and C7) which, thus activated, go on to cleave hundreds of proteins[6] as part of the apoptotic cell death program. The importance of caspases in various cellular processes and disease states emphasizes the potential value of isoform-selective small molecule inhibitors and probes of caspase activity. Historically, small molecule probes (e.g. Ac-VEID-CHO) and drug moleucles (e.g. emricasan) targeting caspases have been structural mimics of caspase substrates bearing electrophilic functionality (e.g., aldehydes or aryloxymethylketones) to engage the catalytic cysteine residue (Figure 1). Although such tools are widely available and frequently used in biomedical research, their lack of significant isoform selectivity, particularly in cellular contexts, confounds the biological or pharmacological conclusions inferred from their use.[7] Moreover, electrophilic substrate mimics have proved challenging to develop clinically,[8,9] likely due to insufficient selectivity and/or sub-optimal drug-like properties.

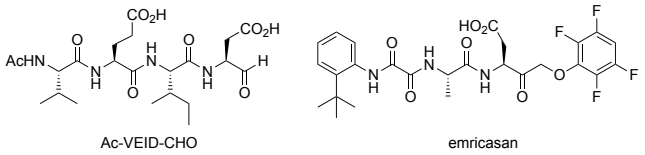

Figure 1. Examples of substrate-like tool compounds and drug candidates that engage the catalytic cysteine of caspases.

While often classified as an executioner caspase, the function of Caspase-6 (C6) in physiology and disease has remained enigmatic and it has been suggested that C6 may act upstream of the other executioner caspases.[4,10] In addition to a putative amplifying role during apoptosis, C6 has been found to also possess nonapoptotic functions important for axon pruning and neuroinflammation.[11–14] Finally, C6-mediated proteolysis has been implicated in the pathology of Huntington's[15,16] and Alzheimer's disease,[17–19] in neuroinflammation generally,[20–22] and in nonalcoholic steatohepatitis (NASH).[14]

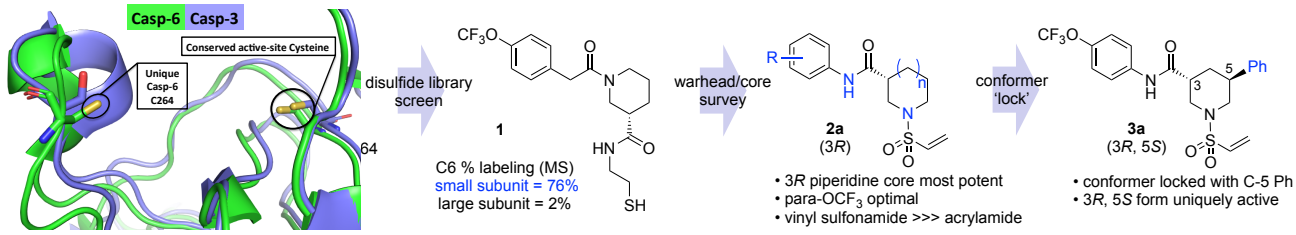

Figure 2. Summary of a targeted approach to the discovery of potent and selective caspase-6 inhibitors and chemical probes.

There is a clear need for potent and selective C6 inhibitors and activity-based probes to validate and exploit the role of C6 in these disease states. To produce the first truly selective probe of C6 activity in cellular contexts, we leveraged a non-conserved cysteine residue (C264) that lies on a loop at the distal end of the active site (Figure 2). Disulfide trapping (tethering[23]) is a now well-established approach to identify covalent probe ligands for surface exposed/reactive cysteines in diverse proteins. Its application to caspases was first reported by Hardy and Wells[24,25] who showed that endogenous cysteine residues found at the dimer interface of C3 and C7 could be trapped as disulfides with small molecule thiols to stabilize an inactive, zymogen-like conformation, thereby inhibiting the protease in biochemical assays. While disulfide probes are generally unsuited for work in cells due to the reducing intracellular environment, this seminal work nevertheless inspired subsequent zymogen-stabilization approaches in other caspases by both covalent[26] and non-covalent means.[16,27] However, small molecule targeting of a caspase *active site* by engaging a non-catalytic residue has not to our knowledge been described previously.

RESULTS and DISCUSSION

C6 possesses a non-catalytic cysteine (C264) not present in other family members and situated on a loop in the small subunit at the distal end of the active site (Figure 2). The catalytic cysteine (C163) is found on the large subunit, while two additional cysteine residues appear to be buried and thus inaccessible for disulfide formation. A disulfide tethering screen of C6 was performed employing our synthetic library of ~1,500 diverse disulfide-bearing small molecules.[28,29] In this technique[30] protein-disulfide conjugates formed under reducing conditions are detected by automated HPLC/MS (Supplementary Figure 1A). Notably, a large majority of screening hits labelled the small subunit, suggesting a preference for C264 over the catalytic cysteine C163 on the large subunit (Supplementary Figure 1B). Moreover, labelling of the small subunit in MS experiments correlated with inhibition of C6 in biochemical assays (Supplementary Figure 1C). The best C264-binding thiols contained a substituted piperidine scaffold with either a 3-amido (derived from nipecotic acid) or 4-amido linkage to the disulfide. The distal substituents varied, including substituted phenyls, 5,6-fused rings, and 6,6-fused rings (Supplementary Figure 1D).

Among the thiol-bearing hits identified in the screen was (*S*)-nipecotic acid-derived analog **1** bearing a distal para-trifluoromethoxy substituted aryl ring (Figure 2). As with the other hits identified in the screen, compound **1** labelled the small subunit almost exclusively. To derive a cell-active probe, we sought to replace the thiol side chain with a suitably positioned, electrophilic warhead. In one successful foray leading to analog **2a** (R = *p*-OCF_3), the nipecotic acid core was retained but with the carboxylic acid used to display the aryl side chain and with the piperidine nitrogen presenting a vinylsulfonamide electrophile. Analog **2a**, having the 3*R* configuration, exhibited markedly superior C264 engagement (dose-response 50; DR_{50} value) and C6 inhibition when compared to its enantiomer **2b** (Scheme 1 and Table 1), indicating that inhibition by **2a** involves both molecular recognition and reaction with C264. Notably, among several cysteine reactive warheads explored in the context of analog **2a**, the vinylsulfonamide alone provided potent C6 inhibition. Also fortuitously, the *para*-trifluoromethoxyaryl ring present in the original screening hit **1** proved superior to many differently substituted aryl rings explored and was thus retained during further optimization.

The crystal structure of **2a** bound to C6 confirmed covalent modification of residue C264, whose α-carbon atom moved ~2.4Å towards the substrate binding groove, compared to the structure of C6 bound to a VEID peptide substrate analog (Figure 3). Guided by this structure, we explored additional substitution of the piperidine ring, seeking to engage additional pockets in the active site. Our modelling suggested this could be achieved with a bulky substituent at the C-5 position bearing a *cis* relationship to the existing benzamide side chain at C-3. Contrary to expectation however, it was the *trans* diastereomer **3-*t*** that confered potent C6 inhibition, while the *cis* diastereomer **3-*c*** was without detectable biochemical activity (Table 1).

To identify the eutomer and distomer of racemic **3-*t***, we separated the enantiomers of the precursor **8-*t*** (Scheme 2) and used these materials to prepare analogs **3a** (*3R*, *5S*) and **3b** (*3S*, *5R*). When tested in a biochemical assay, enantiomer **3a** potently inhibited C6 activity with an IC_{50} value of 7 nM while its enantiomer **3b** exhibited an IC_{50} at least 100-fold weaker (Table 1). X-ray crystallography showed a binding pose with similarities and differences as compared to **2a** (Figure 3A). In both analogs, the trifluoromethoxyaryl side chain was buried in the S1 pocket, where the aspartic acid residue of the C6 substrate is usually bound (Figure 3A). To accommodate this large and hydrophobic ring system, arginine 220, which formed hydrogen bonds with the aspartic acid in VEID peptide type inhibitors, moved by 4.2 Å (ε nitrogen) to create a hydrophobic cavity complementary in shape to the sidechain of **3a** (Figure 3B). By contrast, the location and orientation of the piperidine ring and sulfonamide function was quite different in the two analogs. The phenyl substituent present in **3a** made few if any contacts with protein, but in occupying an equatorial position in the bound conformation, helps to make energetically feasible the required axial orientation of the trifluoromethoxy benzamide side chain bound within the S1 pocket.

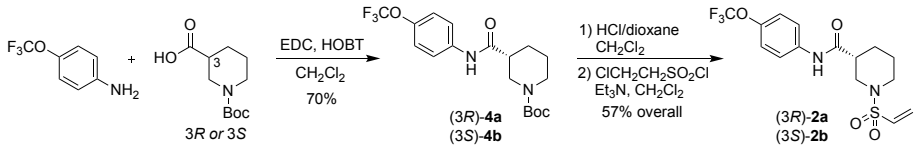

Scheme 1. Synthesis of enantiomers 2a and 2b.

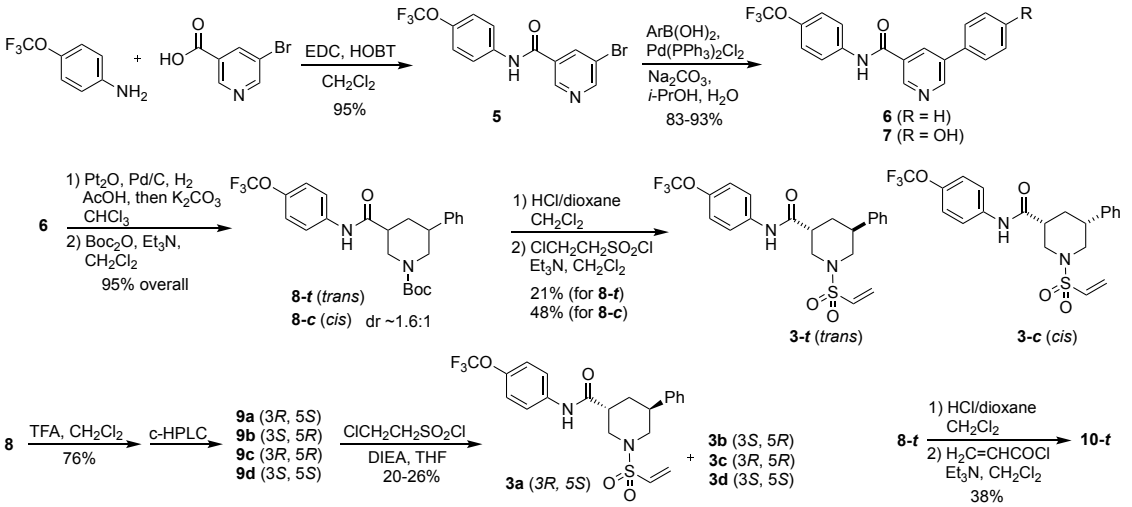

Scheme 2. Synthesis of racemic *trans* **and** *cis* **analogs 3-*t*** and **3-*c***, and non-racemic stereoisomers **3a-d**. The latter were prepared from the individual stereoisomers **9a-d**, which were separated by chiral-HPLC. The acrylamide analog **10-*t*** was synthesized from **8-*t*** as shown at lower right.

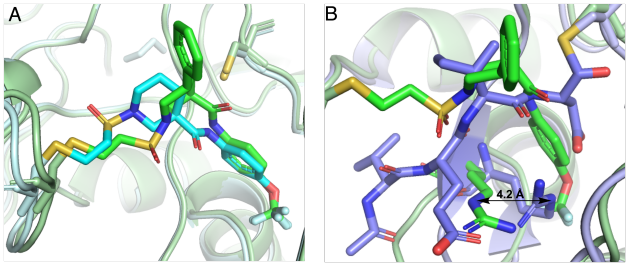

Figure 3. Structures of **2a** and **3a** and Ac-VEID-CHO bound to Caspase-6. A) Superposition of crystal structures of **2a** (cyan) and **3a** (green) bound in the active site of caspase-6. The catalytic cysteine C163 is on the large subunit (at right) while the inhibitor-modified C264 is on the small subunit (at left). B) Superposition of **3a** (green, light green protein) and substrate analog Ac-VEID-CHO (violet, light violet protein). The side chain of R220 moves 4.2 Å to accommodate the trifluoromethoxyphenyl substituent on **3a**. PDBIDs: 8EG6 (**2a**/C6); 8EG5 (**3a**/C6); 3OD5 (VEID/C6).

When **3a** was tested at 10 μM (>100-fold its C6 IC_{50}) against caspases C1 – C10, the compound had little if any effect on any of the other isoforms (Figure 4). The exquisite potency and isoform selectivity of **3a**, together with the lack of C6 activity for its enantiomer **3b**, strongly suggested that **3a** bound C6 in a favorable pre-covalent complex that positioned the electrophilic vinylsulfonamide for subsequent reaction with C264. Interestingly then, the acrylamide **10-*t***, a direct congener of **3-*t*** (Scheme 2) lacked any measurable activity against C6, highlighting the subtleties of covalent ligand design and the importance of properly positioning electrophilic centers for reaction with protein nucleophiles.

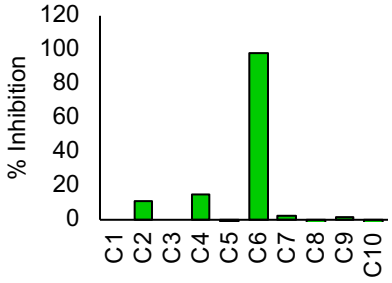

Figure 4. Inhibition of caspase isoforms by 10 μM of **3a**, ca. 100-fold its caspase-6 IC_{50} value. Activity measured by cleavage of aminofluorocoumarin (AFC)-labeled peptides (see Supplementary Information). C = caspase.

To better understand the inhibition of C6 by **3a**, we determined its kinetic parameters (k_{inact}/K_i values) for inhibition (Supplementary Figure 2). This data indicated that indeed, both noncovalent and covalent interactions contributed to the binding of **3a**, with the K_i value of 7.0 μM providing an estimate of the intrinsic pre-covalent binding affinity of **3a** for C6. Moving to cellular studies, **3a** showed potent inhibition of C6 in SK-N-AS, a neuroblastoma cell line.

Table 1. Measures of C264 engagement, biochemical IC_{50} values and inhibition kinetics for Caspase-6 inhibitors.

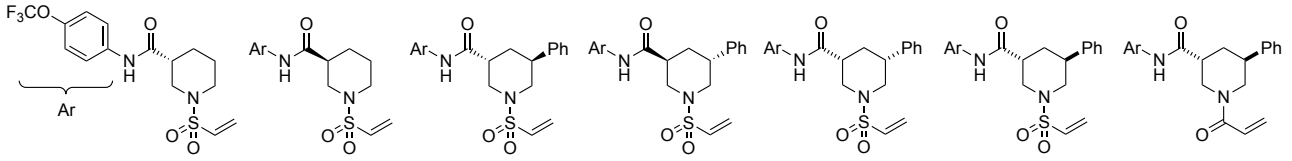

	2a (3*R*)	**2b** (3*S*)	**3a** (3*R*, 5*S*)	**3b** (3*S*, 5*R*)	(±)-**3-*c*** (*cis*)	(±)-**3-*t*** (*trans*)	(±)-**10-*t*** (*trans*)
Casp-6 IC_{50}	0.27 μM	210 μM	0.007 μM	> 10 μM	> 500 μM	0.040 μM	>500 μM
$C6^{sm}$ DR_{50}[a]	0.08 μM	13 μM	-	-	-	-	-
K_i	-	-	7.0 μM	-	-	12.5 μM	-
k_{inact}	-	-	3.1 x 10^{-2} s^{-1}	-	-	1.67 x 10^{-2} s^{-1}	-
k_{inact}/K_i	-	-	4400 M^{-1} s^{-1}	-	-	1,330 M^{-1} s^{-1}	-
Casp-3 IC_{50}	>500 μM	-	> 500 μM	-	>500 μM	>500 μM	-

Table subscript. [a]DR_{50} is the concentration of inhibitor producing 50% labeling of the Casp-6 small subunit ($C6^{sm}$) as determined by MS.

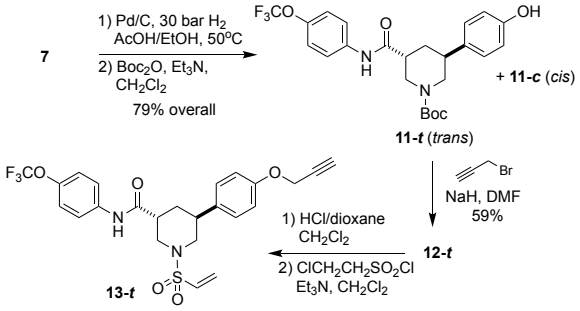

Scheme 3. Synthesis of **13-*t*** a prototype activity-based probe of Caspase-6 for cellular and chemoproteomic studies.

This assay measured C6-mediated cleavage of lamin A, a C6-specific substrate,[31] under staurosporine-induced caspase activation. After 1 hr preincubation with compound and three hours incubation with staurosporine, lamin A cleavage was inhibited by **3a** with an IC_{50} value of 170 nM (Figure 5).

Having established that **3-*t*/3a** exhibits potent and selective C6 inhibition, we next sought to evaluate selectivity in a cellular context where many surface exposed and reactive cysteine thiols are present. We synthesized (±)-*trans*-**13** (**13-*t***), a direct congener of **3-*t*** bearing a propargyl ether substituent on the aryl side chain (Scheme 3). We evaluated the proteome-wide selectivity of this analog in HEK293 cells using stable isotope labeling by amino acids in cell culture (SILAC) quantitative liquid chromatography/mass spectrometry (LC/MS). Since active C6 levels were below our limit of detection for LC/MS in several cell lines (data not shown), we instead transfected HEK293 cells with an autoactivating form of caspase-6. After 24 hrs of transfection, 1μM probe **13-*t*** was added to cells for 60 min, with or without 60 minute pre-treatment with 10 μM **3a** as competitor. Cells were lysed and heavy and light SILAC lysates were combined in a 1-1 ratio, treated with azido-biotin, and subjected to click chemistry to biotinylate probe-labeled proteinsfor subsequent capture on streptavidin-coated beads. Bound proteins were digested on-bead and measured by liquid chromatography/mass spectrometry (LC-MS/MS). Protein levels were compared to cells treated identically, but without addition of **13-*t*** or **3a**. Only eight proteins were significantly enriched in the presence of **13-*t*** (enrichment ≥ 2-fold) while also being competed by **3a**, suggesting specific labeling (Figure 5). The small subunit of C6, which contains C264, was the second-most enriched hit and was highly significant, with p = 10^{-14} (Supplementary Figure 3). By contrast, the large subunit of C6 was not significantly enriched. None of the remaining putative off-targets were proteases; all are membrane-associated proteins, including two heme proteins (CYB5B, HMOX2) and one cysteine-dependent enzyme (PTGES2). These data indicate that **13-*t*** (and by extension **3a**) showed excellent selectivity for C6 across the cellular cysteineome.

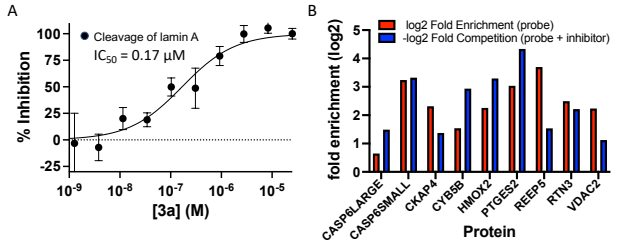

Figure 5. Cell-based activity and selectivity of **3a**. A) Inhibition of lamin A cleavage in SK-N-AS cells after staurosporine induction of caspases. Cells were treated with 3a for 1 hr before addition of 10 μM staurosporine for 4 hrs. B) Targets of **13-*t*** (1 μM) in HEK293 cells transfected with caspase-6, detected by SILAC LC/MS-based proteomics. Graph shows proteins that were a) enriched at least 2-fold by **13-*t*** affinity purification compared to background binding to streptavidin-coated beads (red) and b) at least 2-fold reduced by pretreatment with 10 μM **3a** (blue).

CONCLUSIONS

Here we used disulfide trapping and structure guided covalent ligand design to develop Caspase-6 inhibitors and activity-based probes with unprecedented selectivity over the other

caspase family members and useful selectivity across the cellular proteome. Compared to the peptide electrophiles widely used currently to study caspases in biological contexts, compounds such as **3a** and **13-*t*** better exemplify the characteristics[7] of chemical probes suitable for biomedical research. Beyond their utility as probes, the compounds described herein represent suitable starting points for the future development of potent and isoform-selective caspase-6 inhibitors as therapeutic leads. Efforts in this direction are underway and will be reported in due course.

ASSOCIATED CONTENT

Supporting Information

Experimental procedures and Supplemetary Figures. The Supporting Information is available free of charge on the ACS Publications website.

AUTHOR INFORMATION

Corresponding Authors

Michelle R. Arkin – Department of Pharmaceutical Chemistry, University of California, San Francisco, San Francisco, California, 94143, United States; orcid.org/0000-0002-9366-6770; Email: michelle.arkin@ucsf.edu

Adam R. Renslo – Department of Pharmaceutical Chemistry, University of California, San Francisco, San Francisco, California, 94143, United States; orcid.org/0000-0002-1240-2846; Email: adam.renslo@ucsf.edu

Authors

Kurt Van Horn – Department of Pharmaceutical Chemistry, University of California, San Francisco, San Francisco, California, 94143, United States.

Dongju Wang – Department of Pharmaceutical Chemistry, University of California, San Francisco, San Francisco, California, 94143, United States and School of Pharmaceutical Sciences, Tsinghua University, Beijing, China.

Daniel Medina-Cleghorn – Department of Pharmaceutical Chemistry, University of California, San Francisco, San Francisco, California, 94143, United States.

Peter S. Lee – Department of Pharmaceutical Chemistry, University of California, San Francisco, San Francisco, California, 94143, United States.

Clifford Bryant – Department of Pharmaceutical Chemistry, University of California, San Francisco, San Francisco, California, 94143, United States.

Chad Altobelli – Department of Pharmaceutical Chemistry, University of California, San Francisco, San Francisco, California, 94143, United States.

Priyadarshini Jaishankar – Department of Pharmaceutical Chemistry, University of California, San Francisco, San Francisco, California, 94143, United States.

Kevin K. Leung - Department of Pharmaceutical Chemistry, University of California, San Francisco, San Francisco, California, 94143, United States.

Raymond A. Ng – Formerly Chempartner Corporation. Current address: Olema Oncology, San Francisco, CA.

Andrew J. Ambrose - Department of Pharmaceutical Chemistry, University of California, San Francisco, San Francisco, California, 94143, United States.

Yinyan Tang - Department of Pharmaceutical Chemistry, University of California, San Francisco, San Francisco, California, 94143, United States.

Author Contributions

‡These authors contributed equally to this work.

Notes

The authors declare the following competing financial interest(s): M.R.A. and A.R.R. are co-founders and advisors of Elgia Therapeutics.

ACKNOWLEDGEMENTS

The authors gratefully acknowledge Jie Liu, Yanli Wang, Yanlong Zhao, and Panpan Fan (Viva Biosciences) for re-collection and submission of the structures 8EG5 and 8EG6 to the protein data bank. We are also grateful to Jamie Byrne for mass spectrometry analysis. This research was supported by CHDI (M.R.A. and A.R.R.), the Alzheimer's Association DVT-14-322219 (M.R.A. and A.R.R.), and the National Institutes of Health 1F32AG072822-01 (A.J.A.).

REFERENCES

(1) Thornberry, N. A.; Lazebnik, Y. Caspases: Enemies Within. *Science* **1998**, *281*, 1312–1316.

(2) Green, D. R. Apoptotic Pathways: The Roads to Ruin. *Cell* **1998**, *94*, 695–698.

(3) Wilson, C. H.; Kumar, S. Caspases in Metabolic Disease and Their Therapeutic Potential. *Cell Death Differ.* **2018**, *25*, 1010–1024.

(4) McIlwain, D. R.; Berger, T.; Mak, T. W. Caspase Functions in Cell Death and Disease. *Cold Spring Harb. Perspect. Biol.* **2013**, *5*, a008656.

(5) Graham, R. K.; Ehrnhoefer, D. E.; Hayden, M. R. Caspase-6 and Neurodegeneration. *Trends Neurosci.* **2011**, *34*, 646–656.

(6) Julien, O.; Wells, J. A. Caspases and Their Substrates. *Cell Death Differ.* **2017**, *24*, 1380–1389.

(7) Arrowsmith, C. H.; Audia, J. E.; Austin, C.; Baell, J.; Bennett, J.; Blagg, J.; Bountra, C.; Brennan, P. E.; Brown, P. J.; Bunnage, M. E.; Buser-Doepner, C.; Campbell, R. M.; Carter, A. J.; Cohen, P.; Copeland, R. A.; Cravatt, B.; Dahlin, J. L.; Dhanak, D.; Edwards, A. M.; Frederiksen, M.; Frye, S. V.; Gray, N.; Grimshaw, C. E.; Hepworth, D.; Howe, T.; Huber, K. V. M.; Jin, J.; Knapp, S.; Kotz, J. D.; Kruger, R. G.; Lowe, D.; Mader, M. M.; Marsden, B.; Mueller-Fahrnow, A.; Müller, S.; O'Hagan, R. C.; Overington, J. P.; Owen, D. R.; Rosenberg, S. H.; Roth, B.; Ross, R.; Schapira, M.; Schreiber, S. L.; Shoichet, B.; Sundström, M.; Superti-Furga, G.; Taunton, J.; Toledo-Sherman, L.; Walpole, C.; Walters, M. A.; Willson, T. M.; Workman, P.; Young, R. N.; Zuercher, W. J. The Promise and Peril of Chemical Probes. *Nat. Chem. Biol.* **2015**, *11*, 536–541.

(8) Linton, S. D.; Aja, T.; Armstrong, R. A.; Bai, X.; Chen, L.-S.; Chen, N.; Ching, B.; Contreras, P.; Diaz, J.-L.; Fisher, C. D.; Fritz, L. C.; Gladstone, P.; Groessl, T.; Gu, X.; Herrmann, J.; Hirakawa, B. P.; Hoglen, N. C.; Jahangiri, K. G.; Kalish, V. J.;

Karanewsky, D. S.; Kodandapani, L.; Krebs, J.; McQuiston, J.; Meduna, S. P.; Nalley, K.; Robinson, E. D.; Sayers, R. O.; Sebring, K.; Spada, A. P.; Ternansky, R. J.; Tomaselli, K. J.; Ullman, B. R.; Valentino, K. L.; Weeks, S.; Winn, D.; Wu, J. C.; Yeo, P.; Zhang, C. First-in-Class Pan Caspase Inhibitor Developed for the Treatment of Liver Disease. *J. Med. Chem.* **2005**, *48*, 6779–6782.

(9) Harrison, S. A.; Goodman, Z.; Jabbar, A.; Vemulapalli, R.; Younes, Z. H.; Freilich, B.; Sheikh, M. Y.; Schattenberg, J. M.; Kayali, Z.; Zivony, A.; Sheikh, A.; Garcia-Samaniego, J.; Satapathy, S. K.; Therapondos, G.; Mena, E.; Schuppan, D.; Robinson, J.; Chan, J. L.; Hagerty, D. T.; Sanyal, A. J. A Randomized, Placebo-Controlled Trial of Emricasan in Patients with NASH and F1-F3 Fibrosis. *J. Hepatol.* **2020**, *72*, 816–827.

(10) Creagh, E. M. Caspase Crosstalk: Integration of Apoptotic and Innate Immune Signalling Pathways. *Trends Immunol.* **2014**, *35*, 631–640.

(11) Slee, E. A.; Adrain, C.; Martin, S. J. Executioner Caspase-3, -6, and -7 Perform Distinct, Non-Redundant Roles during the Demolition Phase of Apoptosis. *J. Biol. Chem.* **2001**, *276*, 7320–7326.

(12) Klaiman, G.; Champagne, N.; LeBlanc, A. C. Self-Activation of Caspase-6 in Vitro and in Vivo: Caspase-6 Activation Does Not Induce Cell Death in HEK293T Cells. *Biochim. Biophys. Acta* **2009**, *1793*, 592–601.

(13) Geden, M. J.; Romero, S. E.; Deshmukh, M. Apoptosis versus Axon Pruning: Molecular Intersection of Two Distinct Pathways for Axon Degeneration. *Neurosci. Res.* **2019**, *139*, 3–8.

(14) Zhao, P.; Sun, X.; Chaggan, C.; Liao, Z.; In Wong, K.; He, F.; Singh, S.; Loomba, R.; Karin, M.; Witztum, J. L.; Saltiel, A. R. An AMPK-Caspase-6 Axis Controls Liver Damage in Nonalcoholic Steatohepatitis. *Science* **2020**, *367*, 652–660.

(15) Wong, B. K. Y.; Ehrnhoefer, D. E.; Graham, R. K.; Martin, D. D. O.; Ladha, S.; Uribe, V.; Stanek, L. M.; Franciosi, S.; Qiu, X.; Deng, Y.; Kovalik, V.; Zhang, W.; Pouladi, M. A.; Shihabuddin, L. S.; Hayden, M. R. Partial Rescue of Some Features of Huntington Disease in the Genetic Absence of Caspase-6 in YAC128 Mice. *Neurobiol. Dis.* **2015**, *76*, 24–36.

(16) Ehrnhoefer, D. E.; Skotte, N. H.; Reinshagen, J.; Qiu, X.; Windshügel, B.; Jaishankar, P.; Ladha, S.; Petina, O.; Khankischpur, M.; Nguyen, Y. T. N.; Caron, N. S.; Razeto, A.; Meyer Zu Rheda, M.; Deng, Y.; Huynh, K. T.; Wittig, I.; Gribbon, P.; Renslo, A. R.; Geffken, D.; Gul, S.; Hayden, M. R. Activation of Caspase-6 Is Promoted by a Mutant Huntingtin Fragment and Blocked by an Allosteric Inhibitor Compound. *Cell Chem. Biol.* **2019**, *26*, 1295–1305.e6.

(17) Uribe, V.; Wong, B. K. Y.; Graham, R. K.; Cusack, C. L.; Skotte, N. H.; Pouladi, M. A.; Xie, Y.; Feinberg, K.; Ou, Y.; Ouyang, Y.; Deng, Y.; Franciosi, S.; Bissada, N.; Spreeuw, A.; Zhang, W.; Ehrnhoefer, D. E.; Vaid, K.; Miller, F. D.; Deshmukh, M.; Howland, D.; Hayden, M. R. Rescue from Excitotoxicity and Axonal Degeneration Accompanied by Age-Dependent Behavioral and Neuroanatomical Alterations in Caspase-6-Deficient Mice. *Hum. Mol. Genet.* **2012**, *21*, 1954–1967.

(18) Theofilas, P.; Ehrenberg, A. J.; Nguy, A.; Thackrey, J. M.; Dunlop, S.; Mejia, M. B.; Alho, A. T.; Paraizo Leite, R. E.; Rodriguez, R. D.; Suemoto, C. K.; Nascimento, C. F.; Chin, M.; Medina-Cleghorn, D.; Cuervo, A. M.; Arkin, M.; Seeley, W. W.; Miller, B. L.; Nitrini, R.; Pasqualucci, C. A.; Filho, W. J.; Rueb, U.; Neuhaus, J.; Heinsen, H.; Grinberg, L. T. Probing the Correlation of Neuronal Loss, Neurofibrillary Tangles, and Cell Death Markers across the Alzheimer's Disease Braak Stages: A Quantitative Study in Humans. *Neurobiol. Aging* **2018**, *61*, 1–12.

(19) Theofilas, P.; Piergies, A. M. H.; Oh, I.; Lee, Y. B.; Li, S. H.; Pereira, F. L.; Petersen, C.; Ehrenberg, A. J.; Eser, R. A.; Ambrose, A. J.; Chin, B.; Yang, T.; Khan, S.; Ng, R.; Spina, S.; Seeley, W. W.; Miller, B. L.; Arkin, M. R.; Grinberg, L. T. Caspase-6-Cleaved Tau Is Relevant in Alzheimer's Disease and Marginal in Four-Repeat Tauopathies: Diagnostic and Therapeutic Implications. *Neuropathol Appl Neurobiol* **2022**, *48*, e12819.

(20) LeBlanc, A. C.; Ramcharitar, J.; Afonso, V.; Hamel, E.; Bennett, D. A.; Pakavathkumar, P.; Albrecht, S. Caspase-6 Activity in the CA1 Region of the Hippocampus Induces Age-Dependent Memory Impairment. *Cell Death Differ.* **2014**, *21*, 696–706.

(21) Velagapudi, R.; Kosoko, A. M.; Olajide, O. A. Induction of Neuroinflammation and Neurotoxicity by Synthetic Hemozoin. *Cell Mol. Neurobiol.* **2019**, *39*, 1187–1200.

(22) Angel, A.; Volkman, R.; Royal, T. G.; Offen, D. Caspase-6 Knockout in the 5xFAD Model of Alzheimer's Disease Reveals Favorable Outcome on Memory and Neurological Hallmarks. *Int. J. Mol. Sci.* **2020**, *21*.

(23) Erlanson, D. A.; Braisted, A. C.; Raphael, D. R.; Randal, M.; Stroud, R. M.; Gordon, E. M.; Wells, J. A. Site-Directed Ligand Discovery. *Proc. Natl. Acad. Sci. USA* **2000**, *97*, 9367–9372.

(24) Hardy, J. A.; Lam, J.; Nguyen, J. T.; O'Brien, T.; Wells, J. A. Discovery of an Allosteric Site in the Caspases. *Proc. Natl. Acad. Sci. USA* **2004**, *101*, 12461–12466.

(25) Hardy, J. A.; Wells, J. A. Dissecting an Allosteric Switch in Caspase-7 Using Chemical and Mutational Probes. *J. Biol. Chem.* **2009**, *284*, 26063–26069.

(26) Xu, J. H.; Eberhardt, J.; Hill-Payne, B.; González-Páez, G. E.; Castellón, J. O.; Cravatt, B. F.; Forli, S.; Wolan, D. W.; Backus, K. M. Integrative X-Ray Structure and Molecular Modeling for the Rationalization of Procaspase-8 Inhibitor Potency and Selectivity. *ACS Chem. Biol.* **2020**, *15*, 575–586.

(27) Murray, J.; Giannetti, A. M.; Steffek, M.; Gibbons, P.; Hearn, B. R.; Cohen, F.; Tam, C.; Pozniak, C.; Bravo, B.; Lewcock, J.; Jaishankar, P.; Ly, C. Q.; Zhao, X.; Tang, Y.; Chugha, P.; Arkin, M. R.; Flygare, J.; Renslo, A. R. Tailoring Small Molecules for an Allosteric Site on Procaspase-6. *ChemMedChem* **2014**, *9*, 73–77, 2.

(28) Burlingame, M. A.; Tom, C. T. M. B.; Renslo, A. R. Simple One-Pot Synthesis of Disulfide Fragments for Use in Disulfide-Exchange Screening. *ACS Comb. Sci.* **2011**, *13*, 205–208.

(29) Turner, D. M.; Tom, C. T. M. B.; Renslo, A. R. Simple Plate-Based, Parallel Synthesis of Disulfide Fragments Using the CuAAC Click Reaction. *ACS Comb. Sci.* **2014**, *16*, 661–664.

(30) Hallenbeck, K. K.; Turner, D. M.; Renslo, A. R.; Arkin, M. R. Targeting Non-Catalytic Cysteine Residues Through Structure-Guided Drug Discovery. *Curr. Top. Med. Chem.* **2017**, *17*, 4–15.

(31) Mintzer, R.; Ramaswamy, S.; Shah, K.; Hannoush, R. N.; Pozniak, C. D.; Cohen, F.; Zhao, X.; Plise, E.; Lewcock, J. W.; Heise, C. E. A Whole Cell Assay to Measure Caspase-6 Activity by Detecting Cleavage of Lamin A/C. *PLoS One* **2012**, *7*, e30376.